High-Pass Filtering for Accurate Reconstruction of the Brillouin Frequency Shift Profile From Brillouin Optical Frequency Domain Analysis Data

Luigi Zeni, Ester Catalano, Agnese Coscetta, and Aldo Minardo

Abstract— **In this paper, we propose and demonstrate a new method to reconstruct the Brillouin frequency shift profile in high spatial resolution Brillouin optical frequency domain analysis (BOFDA) sensors. The method aims to compensate the distorting terms affecting BOFDA measurements, which originate from the modulation impressed on the acoustic wave involved in the scattering phenomenon. We show that these terms can be easily removed by applying a high-pass filter to the data acquired in the frequency-domain, at the cost of a degradation of the signal-to-noise ratio. A numerical analysis, as well as experimental tests carried out at 8-mm spatial resolution, validate the proposed technique.**

Index Terms— **Brillouin scattering, optical fiber sensors, strain measurement, temperature measurement.**

I. Introduction

BRILLOUIN Brillouin-based distributed optical fiber sensors have become a consolidated sensing technology due to their ability to measure strain/temperature changes over long distances and with high spatial resolution. In particular, recent progress in the detection schemes have shown that cm-scale or even mm-scale spatial resolution can be reached, which is determinant in numerous applications such as damage detection in structural health monitoring [1] or leak detection in pipelines [2]. In the conventional interrogation method based on the use of a single pump pulse (the so-called Brillouin Optical Time-Domain Analysis, BOTDA), the finite ($\sim$10 ns) build-up time of the acoustic wave involved in the Brillouin scattering process limits the spatial resolution to about 1 m. Therefore, a sub-meter spatial resolution requires the use of more elaborated interrogation schemes. In the time-domain, a differential scheme can be employed (the so-called differential pulse width pair BOTDA, DPP-BOTDA), based on the subtraction of two temporal traces, each of them obtained using long pump pulses of slightly different durations [3]. The pulse widths are large enough to properly build up the acoustic wave, while the resulting spatial resolution is determined by the difference between the pulse widths. An analytical solution for the differential gain in Brillouin optical time-domain analysis reveals that the common-part of the pulse pair provides acoustic wave pre-excitation, while the differential part ensures high spatial resolution [4]. Recently, 1 cm spatial resolution over 10 km in a conventional acquisition time has been demonstrated using an optimized DPP-BOTDA set-up [5]. Other approaches useful for overcoming the limitations due to acoustic wave build up time are pulse pre-pump [6], Brillouin echoes [7], and Brillouin dynamic grating [8]. As an alternative to time-domain schemes, a frequency-domain approach (the so-called Brillouin Optical Frequency-Domain Approach, BOFDA) can be used as well, in which the acoustic wave is pre-excited by the stationary components of the pump and probe fields [9]. As an example, the BOFDA method was recently applied for distributed temperature sensing in polymer optical fibers [10]. In BOFDA, the spatial resolution is obtained by detecting the intensity of light backscattered from a sinusoidally modulated pump, over a proper range of modulation frequencies. Nowadays, the availability of compact and multi-GHz vector network analyzers makes the BOFDA method an attractive solution for the realization of portable interrogation units with cm-scale spatial resolution capabilities. However, the BOFDA method suffers from the presence of distorting terms in the acquired data, which originate from the Brillouin interaction between the stationary component of the pump, and the modulated acoustic wave [11], [12]. These terms must be subtracted from the acquired data; otherwise, the Brillouin frequency shift (BFS) cannot be correctly retrieved in case of non-uniform BFS spatial distribution. In [12], an iterative algorithm has been proposed and demonstrated, in which the exact solution of the Brillouin response of the fiber, when interrogated by a modulated pump, is employed in order to calculate, and then subtract, the distorting terms. The method starts from an approximate estimate of the BFS distribution and then refines this estimate at each iterative step. While effective, this method is computationally intensive, especially when a large number of modulation frequencies and pump/probe frequency shifts are involved. In this paper, we propose a new approximate method, which removes the artefacts from the acquired data by a simple high-pass filtering. Even if approximate, the newly proposed technique is effective in removing the distorting terms, while adding no significant complexity in the BFS profile reconstruction compared to the conventional BOFDA. In the following, we first validate the method by numerical simulations. Then, we apply the technique to experimental

Manuscript received June 26, 2017; revised September 25, 2017; accepted October 26, 2017. Date of publication October 30, 2017; date of current version December 7, 2017. The associate editor coordinating the review of this paper and approving it for publication was Dr. Marco Petrovich. *(Corresponding author: Aldo Minardo.)*

The authors are with the Department of Industrial and Information Engineering, Università della Campania "Luigi Vanvitelli," CAP 81031 Aversa, Italy (e-mail: aldo.minardo@unicampania.it).

Digital Object Identifier 10.1109/JSEN.2017.2768103

data carried out by use of a BOFDA set-up running at 8-mm spatial resolution and under various perturbation profiles.

II. Description of the Method and Numerical Validation

BOFDA sensors are based on the use of a sinusoidally intensity-modulated pump and a continuous wave probe field, which are injected at the opposite ends of the test fiber. If the two optical fields are frequency-shifted of a quantity close to the BFS of the fiber, the stationary components of the optical fields generate, via electrostriction, a stationary acoustic wave that backscatters the pump wave, generating a backscatter signal with the same modulation frequency of the pump. Measuring the amplitude and phase of the alternating part of the back-scattered intensity for a range of modulation frequencies, one achieves the baseband transfer function of the test fiber for a specific pump/probe frequency shift. The pulse response, then, can be simply recovered by calculating the inverse fast Fourier transform (IFFT) of the acquired data. As the backscattered light is generated by a stationary acoustic wave, the recovered Brillouin gain spectrum (BGS) keeps its natural linewidth ($\Delta\upsilon_B \approx$30MHz), independently of the range of modulation frequencies used for data acquisition [11]. Ideally, the pulse response obtained by IFFT resembles the backscatter signal recorded in a BOTDA sensor. Therefore, the BFS can be retrieved after sweeping the pump-probe frequency offset, with a spatial resolution only determined by the bandwidth over which the baseband transfer functions have been acquired, i.e. [9]:

$$\Delta z = \frac{c}{2n}\frac{1}{f_{m,max} - f_{m,min}} \approx \frac{c}{2n}\frac{1}{f_{m,max}} \tag{1}$$

where c is the velocity of light in a vacuum; n is the refractive index of the fiber core; $f_{m,max}$ and $f_{m,min}$ denote the maximum and minimum modulation frequencies, respectively. Such an ideal picture, however, is complicated by the fact that the modulation impressed on the pump field launched into the test fiber inevitably induces some modulation on the electrostrictively-generated acoustic wave. The modulated part of the acoustic wave backscatters the stationary component of the pump wave, producing a spurious signal at the photodetector, which is captured by the network analyzer together with the useful signal. From a mathematical point of view, the overall transfer function is given by [11]:

$$TF(f) = E_{s0}(L)\int_0^L E_{s0}(z)\, g_{B,ac}(z, f)\, e^{-4\pi j f n/c} dz \tag{2}$$

where f is the modulation frequency, L the fiber length, E_{s0} is the stationary probe field, and $g_{B,ac}(z, f)$ is the small-signal Brillouin gain given by:

$$\begin{aligned} g_{B,ac}(z, f) &= \frac{g_{B0}}{2}\left(\frac{1}{1 - j\left(\Delta(z)/\Gamma\right)} + \frac{1}{1 + j\left(\Delta(z)/\Gamma\right)}\right. \\ &\quad + \frac{1}{1 - j\left((\Delta(z) - f)/\Gamma\right)} \\ &\quad \left. + \frac{1}{1 + j\left((\Delta(z) + f)/\Gamma\right)}\right) \end{aligned} \tag{3}$$

In (3), g_{B0} is the peak Brillouin gain coefficient, $\Gamma = \Delta\upsilon_B/2$ is the half-BGS linewidth, $\Delta(z) = \Delta\upsilon_{pp} - BFS(z)$ is the z-dependent detuning, i.e., the difference between the pump/probe frequency shift $\Delta\upsilon_{pp}$and the local BFS. As discussed in [11] and [12], the first two terms in the rhs of (3) describe the backscatter signal generated by the stationary acoustic field (the useful signal), while the last two terms describe the backscatter signal generated by the alternating component of the acoustic field interacting with the stationary pump. In the time domain, the last two terms describe the prolonged backscatter of the pump wave produced by a decaying acoustic wave, even in absence of electrostrictive force. This interaction produces "ghost" peaks in the Brillouin gain spectra, and is responsible for systematic errors in the BFS profile reconstruction in BOFDA sensors [11]. In [12], we have demonstrated an iterative algorithm, which estimate and then subtract these terms from the measurement data. Here, we propose a much faster method based on the simple consideration that the distorting terms scale with $1/f$, while the correct terms do not (see (3)). The physical reason behind this is that, the distorting terms are generated by the modulated component of the acoustic wave, which is naturally low-pass filtered by the inertia of the material [11], while the useful terms are linked to a constant-amplitude modulated pump, which is backscattered by a stationary acoustic field. Based on this consideration, we can set a cut-off frequency, f_c,such that for $f > f_c$ we assume that the distorting terms are null. Instead, for$f < f_c$, we make a further approximation by neglecting the f term in the distorting terms: in this way, the distorting terms are (approximatively) *equal* to the useful terms in this frequency interval. Under such approximations, the distorting term is simply determined by retaining the portion of the measured transfer function up to f_c and attenuating it by 3 dB. Each transfer function can then be corrected (*equalized*) by applying a 3-dB attenuation to the portion of it ranging from $f = f_{m,min}$ to $f = f_c$. In other words, each transfer function is multiplied by a filter function $H(f)$ as follows:

$$TF^{filt}(f) = TF^{unfilt}(f) \cdot H(f) \tag{4}$$

with:

$$H(f) = \begin{cases} \frac{1}{2} & f < f_c \\ 1 & f \geq f_c \end{cases} \tag{5}$$

It is interesting to observe that, the proposed high-pass filtering somewhat resembles the subtraction, performed in DPP-BOTDA sensors, of two Brillouin gain traces acquired with two slightly different pulse durations, where the low-pass spectral portion of the acquired data is associated to the common-part of the pulse pair.

In order to determine the optimal cut-off frequency f_c, we have performed a number of simulations over a 10-m long fiber, having a uniform BFS expect for a central perturbation extending for 20 cm. The modulation frequency was swept from 1 MHz to 1 GHz, ensuring a spatial resolution of 10cm. Note that a 20-cm perturbed length allows the Brillouin gain to reach its maximum at the middle of

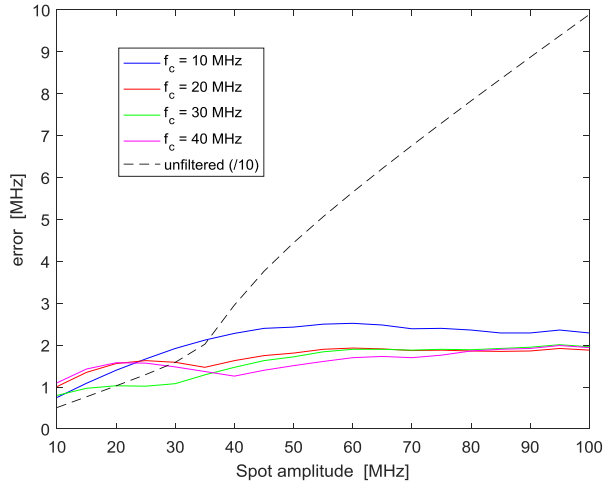

Fig. 1. Maximum deviation between actual and reconstructed BFS profile, at varying amplitudes of the central perturbation and cut-off frequencies. The results for unfiltered data are divided by a factor of 10 for clarity purposes.

the perturbation, when operating at 10-cm spatial resolution. The amplitude of the central perturbation (spot) was varied from 10 MHz to 100 MHz, in terms of BFS shift from the unperturbed fiber. After calculating the transfer functions by use of the model expressed by (3), an IFFT was applied to each unfiltered (or high-pass filtered) transfer function in order to recover the corresponding pulse response. Finally, a curve-fitting procedure was applied to these data in order to determine the BFS distribution in both cases. In Fig. 1, we show the maximum deviation between the actual BFS profile and the reconstructed BFS profile, at varying spot amplitudes and cut-off frequencies. For comparison, we report on the same graph the error in case of standard BOFDA, i.e. by processing the unfiltered transfer functions.

We note that, while the error in standard BOFDA can be as large as 100 MHz (i.e. the central spot is totally missed), the error is always less than 3 MHz when applying the proposed method. Taking into account the average error, the best result is achieved with a cut-off frequency of 30 MHz, with an associated error less than 2 MHz over the entire analyzed range.

In order to appreciate the effect of high-pass filtering, we show in Fig. 2 the time domain Brillouin gain as a function of position and frequency, computed in case of a spot amplitude of 50 MHz, and by taking the IFFT of the unfiltered or filtered transfer functions (with $f_c = 30MHz$). The same figures also display, superimposed, the BFS distribution achieved by curve-fitting the underlying data. Evidently, the two reconstructions differ significantly only in the middle of the fiber, i.e. at the perturbed location.

It is useful to compare the BGS at the perturbed section (Fig. 3). We see that the BGS of the unfiltered BOFDA has two peaks, a first one (slightly higher) centered at the BFS of the unperturbed fiber, and a second one centered at the BFS of the perturbed fiber (i.e. shifted by 50 MHz from the unperturbed fiber). As discussed before, the spurious peak is due to backscatter of the pump from the modulated acoustic wave, and is responsible for the systematic errors

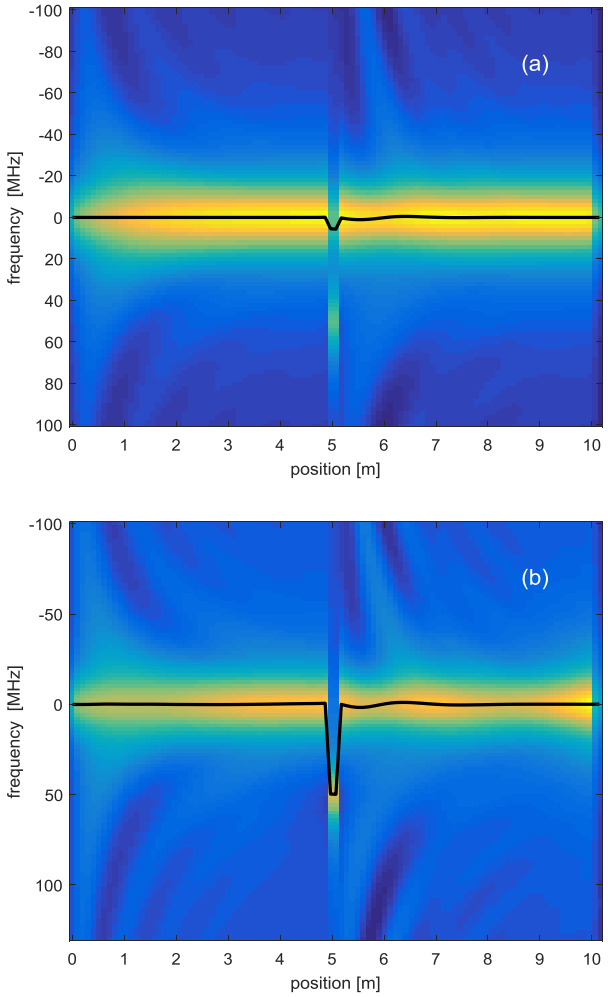

Fig. 2. Brillouin gain map as computed by inverse Fourier transforming the numerically computed, unfiltered transfer functions (a) or the high-pass filtered ones with $f_c = 30MHz$ (b). The black lines show the BFS distribution obtained by curve-fitting the time-domain data.

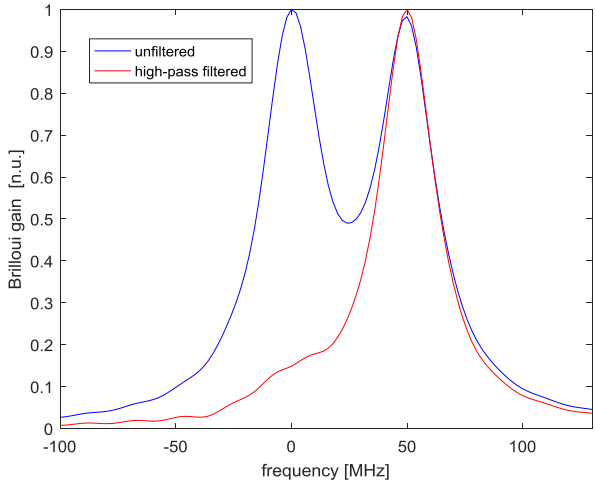

Fig. 3. BGS computed at the middle of a 50-MHz perturbation, using the unfiltered transfer functions (blue line) or the high-pass filtered transfer functions with $f_c = 30MHz$ (red line).

shown in Fig. 2. Instead, the BGS obtained after high-pass filtering shows only one dominant peak, centered at the correct BFS.

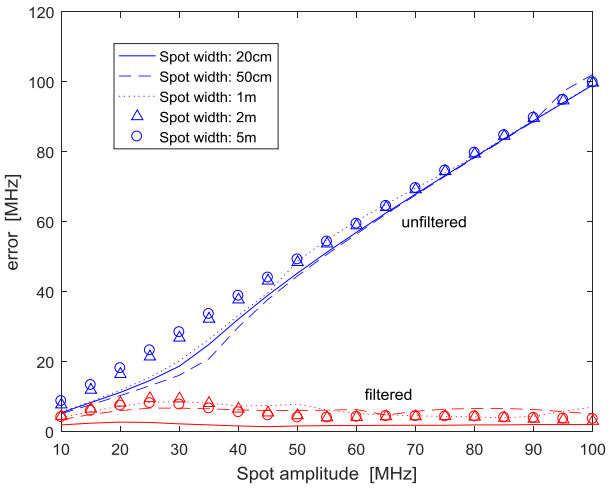

Fig. 4. Maximum deviation between actual and reconstructed BFS profile, at varying amplitudes and widths of the central perturbation.

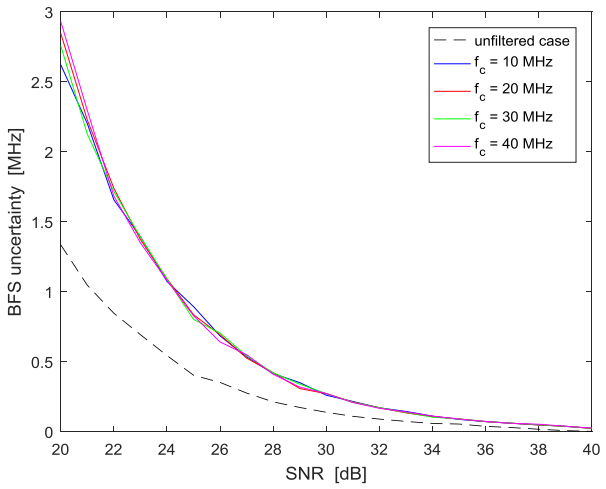

Fig. 5. BFS uncertainty calculated at varying SNR and high-pass cut-off frequencies.

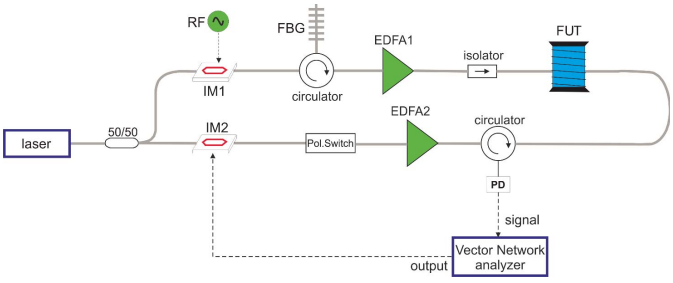

Fig. 6. Experimental setup. IM, intensity modulator; FBG, fiber-Bragg grating; EDFA, erbium-doped fiber amplifier; Pol. Switch, polarization switch; PD, photodetector; FUT, fiber under test.

It is useful to assess the validity of the proposed method also for BFS profiles with a larger low-frequency content. To this aim, we have performed new simulations over a 10-m long fiber, with an increasingly wide central perturbation. We report in Fig. 4 the maximum deviation between the actual BFS profile and the reconstructed BFS profile, by either applying or not the high-pass filtering method, at varying spot amplitudes and for a spot width from 20cm to 5m. The high-pass filtering method was applied with a cut-off frequency $f_c = 30MHz$. We see that, in the filtered case the error increases with the spot width, reaching a maximum of ≈9.5 MHz for a spot amplitude of ≈30 MHz and a width of 2m. Increasing the width further does not influence significantly the quality of reconstruction, as the effect of acoustic wave damping only extends for about 1m after the beginning of the perturbation. The reduced quality of the reconstructed profiles at wider perturbation spots can be explained by considering that, increasing the spot width the amount of low-frequency energy in the transfer functions increases, so that the high-pass filtering of the useful terms (first two terms of Eq. (2)), which is a side effect of the proposed method, becomes more and more important.

However, we also note from Fig. 4 that the high-pass filter method is still effective in improving the quality of reconstruction, even with wider spots, compared to the unfiltered case.

Another side effect of the high-pass filtering is the degradation of the signal-to-noise ratio, with consequent increase of the BFS uncertainty. In fact, assuming that noise spreads uniformly over the whole modulation frequency range, and that most of the energy in the acquired transfer functions is contained in the low-frequency portion (uniform or almost-uniform BFS profiles), attenuating the spectral components from 0 to f_c by 3-dB will reduce the SNR by the same quantity. To confirm this, we have performed a number of simulations over a 10-m long, uniform fiber, in which the transfer functions were computed up to 1 GHz, and artificially corrupted with additive white Gaussian noise (AWGN). We report in Fig. 5 the standard deviation of the BFS profile, calculated at varying SNR and cut-off frequencies (note that the SNR in the horizontal axis refers to the transfer functions before high-pass filtering). As expected, the BFS uncertainty scales with the inverse of the SNR [13]. Furthermore, when applying the high-pass filtering the BFS uncertainty curves are substantially independent of the cut-off frequency, and translated horizontally by 3-dB compared to the unfiltered case. In other words, the BFS uncertainty doubles after application of the high-pass filtering method.

III. Experimental Results

The proposed method has been experimentally assessed by use of the BOFDA scheme shown in Fig. 6. The scheme implements a conventional BOFDA sensor: first, the light from an external cavity laser, with a linewidth less than 100 kHz, is split into distinct branches for pump/probe generation. In the upper (probe) branch, the laser beam is double-sideband (DSB) modulated by means of an intensity electro-optic modulator (IM1) driven by an RF synthesizer. The upper sideband is filtered out by means of a narrowband (≈4 GHz) fiber Bragg grating (FBG), while the lower sideband is amplified by an EDFA (EDFA1) and then launched into one end of the fiber under test (FUT). In the lower (pump) branch, the laser beam is modulated by means of another electro-optic modulator (IM2),

biased at its quadrature point and driven by the RF output of the vector network analyzer (VNA). The modulated pump passes through a polarization switch, which implements a polarization diversity scheme aimed to suppress the polarization dependence of the BGS measurements. Finally, the probe beam is amplified by another EDFA (EDFA2) and launched into the opposite end of the FUT. The backscattered light produced by the pump is fed into a high-bandwidth (12 GHz) photodetector. The VNA covers the range from 300 kHz to 20 GHz, thus permits to investigate the Brillouin response over a maximum fiber length of $\approx$ 300m and with a spatial resolution as high as 5mm.

In order to analyze the performance of the above-explained technique, BOFDA measurements have been carried out over different fibers. As a first test, we have chosen a 23-m fiber length having a nominal BFS of 10690 MHz, along which a short (8mm) segment of fiber with a BFS of 10858MHz was fusion spliced. The frequency of the VNA was swept from 950 kHz to 12161 MHz (12801 frequencies), giving rise to a nominal spatial resolution of $\approx$ 8mm, while the resolution bandwidth (RBW) of the VNA was set to 100 kHz. In order to increase the signal-to-noise ratio, a number of 20 averages was performed for each measured transfer function (ten averages for each one of the two states of the polarization switch). The microwave frequency applied to IM1 was swept from 10650 MHz to 10900 MHz at 2 MHz step, corresponding to 126 transfer functions. As with the numerical analysis, it is useful to compare the IFFT of the unfiltered transfer functions (Fig. 7(a)), with the IFFT of the filtered transfer functions with $f_c = 30MHz$ (Fig. 7(b)). The images are superimposed to the BFS reconstructions obtained by curve-fitting the underlying data. Clearly, the acquired data reveal the short segment of the spliced fiber only after high-pass filtering of the transfer functions.

In Figure 8 we compare the BGS at the perturbed section (located at z$\approx$4.2m along the fiber) before and after high-pass filtering. It is evident that, in the original, unfiltered data the spurious peak is larger than the correct one, which leads to an incorrect estimation of the BFS. Instead, in the filtered data the spurious peak is strongly attenuated, with the BGS now exhibiting only one dominant peak at the correct BFS. The BFS reconstructions, shown in Fig. 7, also reveal some increase of the BFS oscillations along the unperturbed fiber, after application of the high-pass filtering. This is associated to a reduction of the signal-to-noise-ratio (SNR) consequent to the high-pass filtering procedure, as predicted by the simulations shown in previous paragraph. In particular, the standard deviation of the BFS along the unperturbed fiber is 0.98 MHz before high-pass filtering and 1.7 MHz after high-pass filtering. That roughly corresponds to a degradation of the SNR by 3-dB, which is consistent with the numerical results.

As a next step, we have performed a new test in which a 12m-long fiber was heated in five different locations, by placing it in contact with a 2cm-wide resistive heater. The distance between consecutive hot spots was $\approx$ 4 cm. The temperature of the heater was 120 °C, while the rest of the fiber was kept at room temperature ($\approx$20 °C). BOFDA measurements were carried out using the same measurement

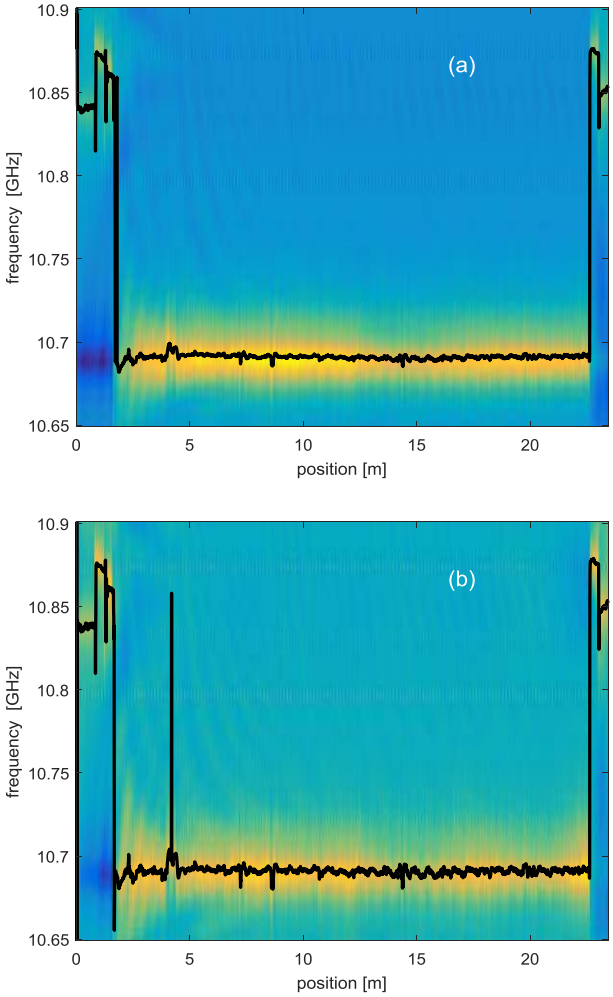

Fig. 7. Brillouin gain map as computed by inverse Fourier transforming the experimental, unfiltered transfer functions (a) or the high-pass filtered ones (b) with $f_c = 30MHz$. The black lines show the BFS distribution obtained by curve-fitting the time-domain data. The regions at the beginning and at the end of the fibers, exhibiting a different BFS, are instrumental.

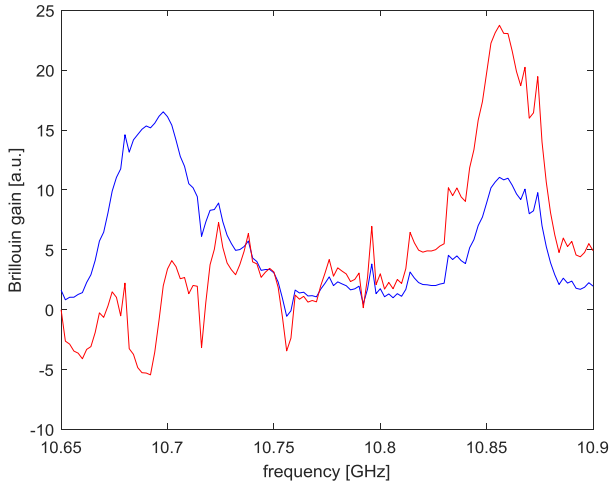

Fig. 8. BGS acquired at the 8-mm spliced fiber segment, using the unfiltered transfer functions (blue line) or the high-pass filtered transfer functions with $f_c = 30MHz$ (red line).

parameters of the previous test. Still, we compare in Fig. 9 the data before and after high-pass filtering. The figures show that, while the reconstruction based on the unfiltered data

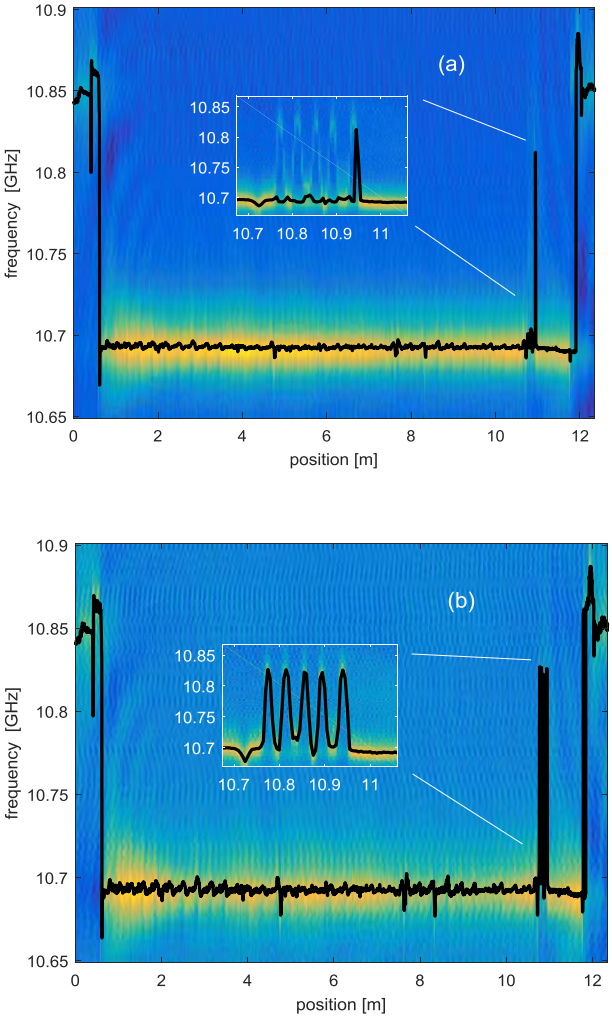

Fig. 9. Brillouin gain map as computed by inverse Fourier transforming the experimental unfiltered transfer functions (a) or the high-pass filtered ones (b) with $f_c = 30MHz$. The black lines show the BFS distribution obtained by curve-fitting the time-domain data. The regions at the beginning and at the end of the fibers, exhibiting a different BFS, are instrumental. The insets show a zoomed view of the perturbed region.

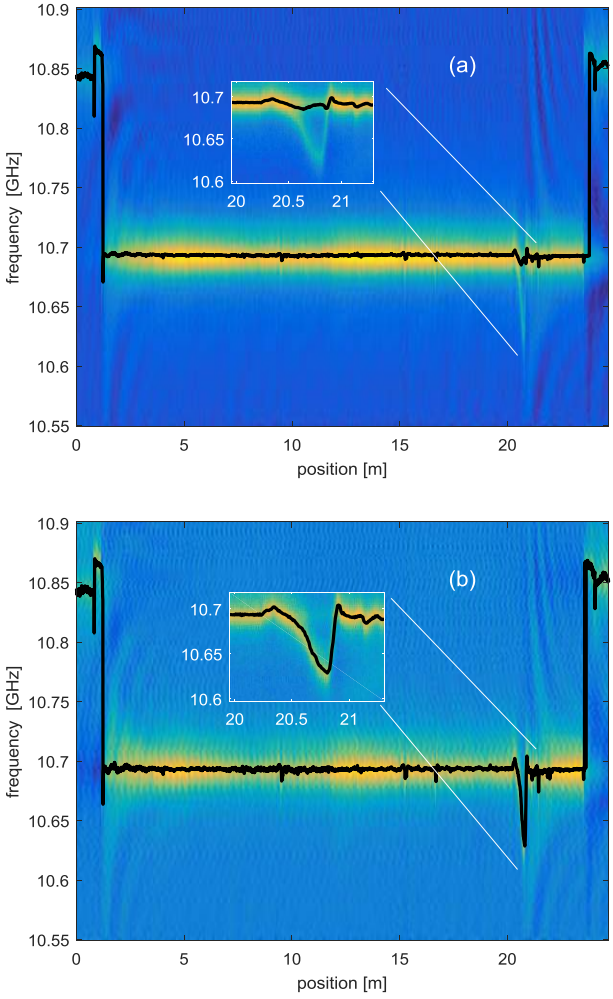

Fig. 10. Brillouin gain map as computed by inverse Fourier transforming the experimental unfiltered transfer functions (a) or the high-pass filtered ones with $f_c = 30MHz$ (b). The black lines show the BFS distribution obtained by curve-fitting the time-domain data. The regions at the beginning and at the end of the fibers, exhibiting a different BFS, are instrumental. The insets show a zoomed view of the perturbed region.

only capture one (out of five) hot spot, the filtered data correctly identifies the entire sequence of hot spots. As already discussed, the incorrect reconstruction of the BFS profile when processing the unfiltered data is a consequence of the spurious peak in the BGS caused by prolonged interaction of the acoustic wave with the pump. Interestingly enough, the classical reconstruction only captures the furthermost hot spot, where the interaction of the pump with the acoustic wave of frequency $\approx$ 10690 MHz is mostly damped.

Still, it is useful to provide the BFS standard deviation outside the perturbed regions. In this case, the standard deviation increases from 1.1 MHz (unfiltered data) to 2.2 MHz (filtered data). Still, that corresponds to a degradation of the SNR by 3-dB, which is consistent with the numerical results.

The last experiment was carried out in conditions of gradual (rather than step-like) spatial changes of the BFS. To this aim, a piece of the fiber was glued along a 70-cm long cantilever beam subjected to deflection. It is well known that the longitudinal strain of the cantilever is maximum at its fixed end, while decreasing linearly when moving toward the free end. In our case, the fiber was glued along the inward face of the cantilever, therefore was subjected to compressive strain.

Figure 10 reports the usual quantities. Again, we see that the filtered data are able to provide the correct distribution of the BFS, which corresponds to a linear strain distribution with a maximum deformation of about 1250 $\mu\varepsilon$ at the fixed end. The efficiency of the proposed method in removing the spatial resolution-degrading features is best appreciated comparing the 3-D distribution of the Brillouin gain in the cantilever region, before and after application of the high-pass filter (see Fig. 11). We see that the ghost peaks, which dominate the Brillouin gain spectra along the cantilever region, are completely suppressed by the high-pass filtering of transfer functions. The same figure also confirms an increase of the background noise consequential to the application of the high-pass filtering. From a quantitative point of view, the standard

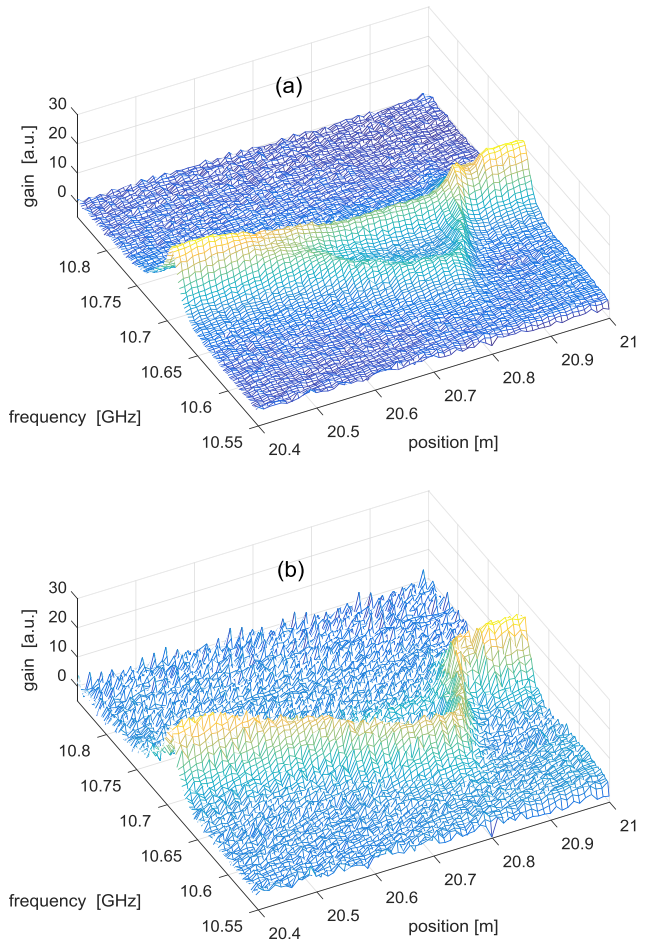

Fig. 11. Brillouin gain map in the perturbed region, as computed by inverse Fourier transforming the experimental, unfiltered transfer functions (a) or the high-pass filtered ones with $f_c = 30MHz$ (b).

deviation of the BFS along the unperturbed fiber is 0.61 MHz in the unfiltered case and 1.25 MHz in the filtered case, confirming the $\approx$ 3-dB SNR degradation. It is worth to mention that, in all considered test cases, the application of the "exact" method described in [7] would have required a processing time in the order of a few hours, while the proposed method does not introduce any significant computation overhead compared to the classical reconstruction method.

IV. CONCLUSION

A high-pass filtering of the data acquired in the frequency-domain has been proposed for suppression of the distorting terms affecting BOFDA measurements and arising from acoustic wave modulation. Compared to our previous method based on the calculation of the distorting terms in iterative steps [8], the method proposed here does not require any integral computation nor iterative procedure, and can be even applied in real-time during the acquisition of the transfer function by proper VNA calibration or customization of its firmware. On the other hand, it has been numerically and experimentally verified that the application of the high-pass filtering method also leads to some degradation of the signal-to-noise ratio (3-dB in case of uniform fiber).

We believe that the presented result is beneficial for a widespread application of the BOFDA technique for high-resolution, medium range distributed optical fiber sensors.

REFERENCES

[1] S. Minakuchi, Y. Okabe, T. Mizutani, and N. Takeda, "Barely visible impact damage detection for composite sandwich structures by optical-fiber-based distributed strain measurement," *Smart Mater. Struct.*, vol. 18, no. 8, p. 085018, 2009.

[2] M. Nikles, "Long-distance fiber optic sensing solutions for pipeline leakage, intrusion, and ground movement detection," *Proc. SPIE*, vol. 7316, pp. 731602–731613, Apr. 2009.

[3] W. Li, X. Bao, Y. Li, and L. Chen, "Differential pulse-width pair BOTDA for high spatial resolution sensing," *Opt. Exp.*, vol. 16, no. 26, pp. 21616–21625, 2008.

[4] A. Minardo, R. Bernini, and L. Zeni, "Differential techniques for high-resolution BOTDA: An analytical approach," *IEEE Photon. Technol. Lett.*, vol. 24, no. 15, pp. 1295–1297, Aug. 1, 2012.

[5] A. Dominguez-Lopez, M. A. Soto, S. Martin-Lopez, L. Thevenaz, and M. Gonzalez-Herraez, "Resolving 1 million sensing points in an optimized differential time-domain Brillouin sensor," *Opt. Lett.*, vol. 42, no. 10, pp. 1903–1906, 2017.

[6] K. Kishida, C.-H. Li, and K. Nishiguchi, "Pulse pre-pump method for cm-order spatial resolution of BOTDA," *Proc. SPIE*, vol. 5855, pp. 559–562, May 2005.

[7] L. Thévenaz and S. F. Mafang, "Distributed fiber sensing using Brillouin echoes," *Proc. SPIE*, vol. 7004, p. 70043N, May 2008.

[8] K. Y. Song, S. Chin, N. Primerov, and L. Thevenaz, "Time-domain distributed fiber sensor with 1 cm spatial resolution based on Brillouin dynamic grating," in *J. Lightw. Technol.*, vol. 28, no. 14, pp. 2062–2067, Jul. 15, 2010.

[9] D. Garus, T. Gogolla, K. Krebber, and F. Schliep, "Distributed sensing technique based on Brillouin optical-fiber frequency-domain analysis," *Opt. Lett.*, vol. 21, no. 17, pp. 1402–1404, 1996.

[10] A. Minardo, R. Bernini, and L. Zeni, "Distributed temperature sensing in polymer optical fiber by BOFDA," *IEEE Photon. Technol. Lett.*, vol. 26, no. 4, pp. 387–390, Feb. 15, 2014.

[11] A. Minardo, G. Testa, L. Zeni, and R. Bernini, "Theoretical and experimental analysis of Brillouin scattering in single-mode optical fiber excited by an intensity- and phase-modulated pump," *J. Lightw. Technol.*, vol. 28, no. 2, pp. 193–200, Jan. 15, 2010.

[12] R. Bernini, A. Minardo, and L. Zeni, "Distributed sensing at centimeter-scale spatial resolution by BOFDA: Measurements and signal processing," *IEEE Photon. J.*, vol. 4, no. 1, pp. 48–56, Feb. 2012.

[13] M. A. Soto and L. Thévenaz, "Modeling and evaluating the performance of Brillouin distributed optical fiber sensors," *Opt. Exp.*, vol. 21, no. 25, pp. 31347–31366, 2013.

Luigi Zeni received the degree (*summa cum laude*) in electronic engineering from the University of Naples in 1988 and the Ph.D. degree in electronics and computer science from the Italian Ministry of University in 1992. He was with the Delft Institute of Microelectronics and Submicrontechnology, TU-Delft, The Netherlands, as a Visiting Scientist. He is currently a Full Professor of Electronics with the University of Campania Luigi Vanvitelli and the President of the Research Consortium on Advanced Remote Sensing Systems. From 2001 to 2012, he was the Vice Director of the Department of Information Engineering. He is author of more than 135 papers in international journals and more than 140 publications at international conferences. He holds ten patents. He is also the Founder of the spinoff company Optosensing, which deals with structural and environmental monitoring by distributed optical fiber sensors. He has been the national coordinator of PRIN projects, funded by the Italian Ministry of University and Research, in 2000 and 2005, and has been the scientific coordinator of research contracts with public and private institutions and responsible for projects funded within the 7th Framework Program of the European Union. His research interests include the design and realization of optical fiber sensors for distributed measurements of deformation and temperature, the design and characterization of optoelectronic devices with particular emphasis on silicon optoelectronics, optoelectronic integrated sensors, biosensors, and optofluidics, and the design and realization of pulse forming networks for bioelectric applications. He has been a member of the Management Committee of the COST 299 "Optical fibers for new challenges facing the information society" and the COST TD1001 Novel and Reliable Optical Fiber Sensor Systems for Future Security and Safety Applications.

Ester Catalano, photograph and biography not available at the time of publication.

Agnese Coscetta, photograph and biography not available at the time of publication.

Aldo Minardo was born in Naples, Italy, in 1974. He received the Laurea (*summa cum laude*) degree in electronic engineering from the University of Naples Federico II, Naples, Italy, in 2000, and the Ph.D. in electronic engineering from the Second University of Naples, Aversa, Italy, in 2003. He is currently an Associate Professor with the Università della Campania Luigi Vanvitelli. He author of about 200 international journal and conference papers and three patents. He is also the Co-Founder of the spinoff company Optosensing, which deals with structural and environmental monitoring by distributed optical fiber sensors. His main research interests include distributed and point optical fiber sensors. He was responsible for scientific research conventions with private bodies and European projects under the 7th Framework and Horizon 2020 Programs. He received the Best Doctoral Thesis Award in Optoelectronics from the IEEE-LEOS Italian Chapter in 2005. He is a reviewer for several technical journals.